Downloaded from rsta.royalsocietypublishing.org

PHILOSOPHICAL TRANSACTIONS OF THE ROYAL SOCIETY A MATHEMATICAL, PHYSICAL & ENGINEERING SCIENCES

Spatial Resolution in X-Ray Photoelectron Spectroscopy [and Discussion]

I. W. Drummond and R. M. D. Bryson

Phil. Trans. R. Soc. Lond. A 1996 **354**, 2667-2682
doi: 10.1098/rsta.1996.0122

Email alerting service

Receive free email alerts when new articles cite this article - sign up in the box at the top right-hand corner of the article or click **here**

To subscribe to *Phil. Trans. R. Soc. Lond. A* go to:
http://rsta.royalsocietypublishing.org/subscriptions

This journal is © 1996 The Royal Society

Downloaded from rsta.royalsocietypublishing.org

Spatial resolution in X-ray photoelectron spectroscopy

By I. W. Drummond

Kratos Analytical Ltd, Wharfside, Trafford Wharf Road, Manchester M17 1GP, UK

X-ray photoelectron spectroscopy (XPS) is a well established surface analytical technique capable of giving elemental and chemical state information for nearly all elements. Recent improvements in the sensitivity of the method have made spatially resolved XPS a viable technique with, at present, a resolution of 5–30 μm in commercial instrumentation.

The different methods are described and their application to semiconductor devices and materials is outlined with reference to spatial resolution and information in depth. Future prospects for imaging XPS are briefly discussed.

1. Introduction

X-ray photoelectron spectroscopy (XPS) is a relatively recent analytical method (the first commercial instruments became available in 1969) and has yet to achieve a spatial resolution equal to the smallest fabricated detail in semiconductor devices. While the semiconductor industry strives 'Toward "point one" ' (Stix 1995), i.e. a transistor gate length of 0.1 μm, the best available commercial XPS lateral resolution lies in the range 5–30 μm (a conservative figure). Presently most surface microanalytical work on semiconductor devices has been carried out by Auger electron spectroscopy (AES: see Ferguson 1989; Prutton 1996) and secondary ion mass spectrometry (SIMS), both techniques currently having a better spatial resolution than XPS.

However, as will be shown, XPS readily yields chemical information which is much more difficult, if not impossible, to extract from either AES or SIMS and it is for this reason that XPS has a role to play in three-dimensional analysis of semiconductor devices and materials.

In this paper a brief outline of the XPS method will be given and this will be followed by a more detailed study of XPS instrumentation which yield spatial information—particularly information in the plane of the surface of the specimen, although the ability of the method to extract information below the surface (i.e. depth information) will not be overlooked.

2. XPS: the method and spectral information

(*a*) *The method*

XPS is the study of the energy spectrum of electrons emitted by materials when bombarded by X-rays. The history of this study is an exciting one and has been excellently covered by Jenkin and his co-workers (1977, 1978).

Phil. Trans. R. Soc. Lond. A (1996) **354**, 2667–2682
Printed in Great Britain

© 1996 The Royal Society
TEX Paper

The Royal Society is collaborating with JSTOR to digitize, preserve, and extend access to *Philosophical Transactions: Mathematical, Physical and Engineering Sciences.* www.jstor.org

Downloaded from rsta.royalsocietypublishing.org

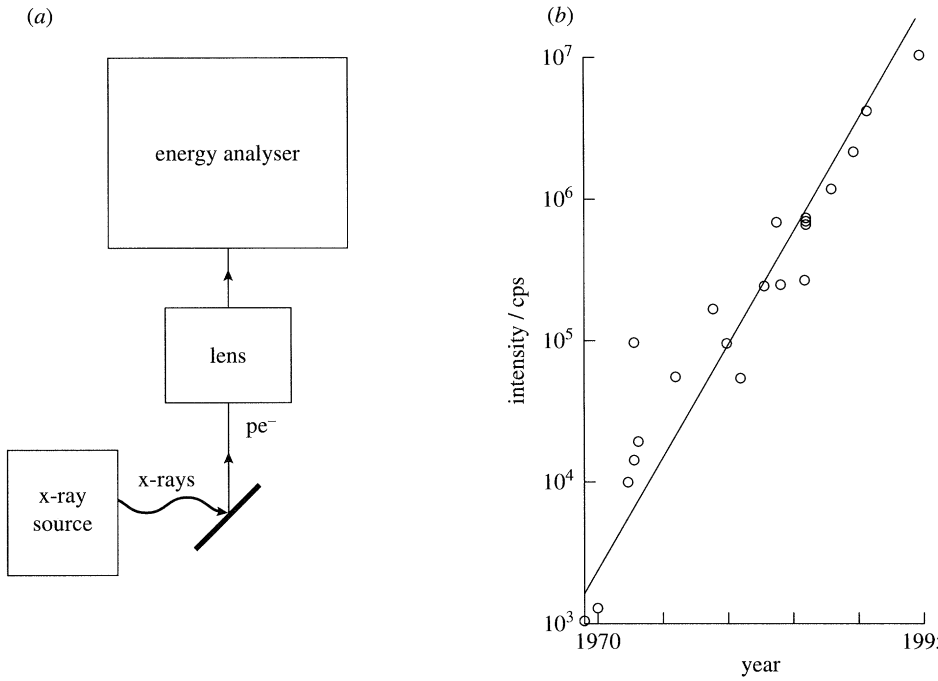

Figure 1. (*a*) Schematic of a basic XPS instrument. (*b*) Increase in sensitivity of commercial XPS instruments during the period 1969 to 1995. The sensitivity is based on the intensity of the Ag(3d) photoelectron peak under a given set of conditions (1 eV FWHM; MgK X-rays: 300 W).

Modern XPS effectively started with a thorough investigation of the method plus significant improvements in the experimental approach by Siegbahn and his co-workers at the University of Uppsala (Siegbahn *et al.* 1967).

The Uppsala group showed that elements could be identified readily by their binding energies but more importantly they showed that small energy perturbations in the binding energy, a so-called 'energy shift', gave an indication of the chemical state(s) of the element. It was this 'chemical shift' which first attracted chemists to the technique. Instrument manufacturers were quick to respond with some five different commercial instruments becoming available in 1969–1970.

In the early 1970s it was soon realized that the strength of XPS lay in surface chemistry, the analytical information coming from the top few atomic layers (i.e. a layer *ca.* 1–6 nm thick). This is because of the limited escape depth of the photoelectrons which, typically, have kinetic energies between 10 and 1500 eV. Experimental results collated by Seah & Dench (1979) show that electrons with energies lying between 10 and 1500 eV have attenuation lengths lying between two and eight atomic layers with a minimum at *ca.* 30 eV.

A schematic of a basic instrument is shown in figure 1*a* while figure 1*b* indicates the improvement in sensitivity of commercial instruments in the last 26 years. The recent increase in sensitivity has led to the development of spatially resolved XPS.

The X-ray source is generally an electron bombardment type configured to produce either MgKα or AlKα on command. Aluminium and magnesium have narrow characteristic lines and AlKα has the advantage that it can be readily monochromated as will be seen in § 3. The emitted photoelectrons from the sample are then focused (often with some retardation) into an energy analyser which is generally

Downloaded from rsta.royalsocietypublishing.org

of the electrostatic hemispherical type. After energy analysis the electrons are detected by an electron multiplier array and recorded by a suitable electronics/data system. The X-ray source, specimen, lens, spectrometer and detector are all housed in a ultra-high vacuum environment so as to minimize contamination of the sample surface.

(*b*) *XPS spectral information*

XPS is essentially a core electron spectroscopy (Woodruff & Delchar 1986), i.e. the peaks in the spectrum correspond to the photoionization of the inner electron shells of the elements present in the surface of the sample. However, information derived from valence electrons can, and is, studied. To a first order, the kinetic energy of the photoelectron can be written as

$$E_k = h\nu - E_{\mathrm{B}}, \tag{2.1}$$

where E_k is the kinetic energy of the emitted photoelectron (eV), $h\nu$ is the energy of the X-ray photon (eV), and E_{B} is the binding energy of the emitted photoelectron (eV). According to Jenkin *et al.* (1977) this expression was first deduced by Rutherford, although not in this form. A more accurate form of the above expression is

$$E_k = h\nu - E_{\mathrm{B}} - \phi, \tag{2.2}$$

where the quantities are the same as in (2.1) but the work function of the spectrometer (ϕ) is taken into account (see Siegbahn *et al.* 1967). Other forms of expression (2.2) exist which take other factors into account but the effects are small and are generally ignored. For further discussions see Woodruff & Delchar (1986) and Watts (1994).

Examination of expression (2.2) shows that if the kinetic energy of the photoelectron is measured and $h\nu$ and ϕ are known then the binding energy of a particular energy level can be determined. Binding energies are well known and the relevant element is easily identified.

The general form of an X-ray photoelectron spectrum is shown in figure 2 which shows a wide scan of silicon with a thin oxide layer. Various photoelectron peaks are observed, e.g. O1s, Si2p, resulting from the photoionization of the O1s and Si2p electron levels, respectively. The Si2p region is shown in more detail where there are two main peaks, one being the Si2p due to Si metal, the other Si2p due to SiO_2. The energy difference between them is *ca.* 4.0 eV and is an example of a chemical shift. The Si2p (metal) peak shows the partially resolved $2p_{1/2}2p_{3/2}$ spin orbit doublet.

Note the oxygen KLL Auger peak which results from the filling of the oxygen K-shell vacancy; an L-shell electron fills the vacancy while another L-shell electron (the Auger electron) is emitted. A competing process can also fill the K-shell vacancy; an L-shell electron fills the K-shell vacancy with simultaneous emission of an X-ray—this is the X-ray fluorescence effect. On the low kinetic energy side of the Si2s and Si2p photoelectron lines there are energy loss structures; in this case they correspond to bulk and surface plasmons of the Si. Other features are found in XPS spectra but they are not discussed here (the interested reader is referred to Briggs & Riviere (1990)).

PHILOSOPHICAL TRANSACTIONS OF THE ROYAL SOCIETY A MATHEMATICAL, PHYSICAL & ENGINEERING SCIENCES
PHILOSOPHICAL TRANSACTIONS OF THE ROYAL SOCIETY A MATHEMATICAL, PHYSICAL & ENGINEERING SCIENCES

Downloaded from rsta.royalsocietypublishing.org

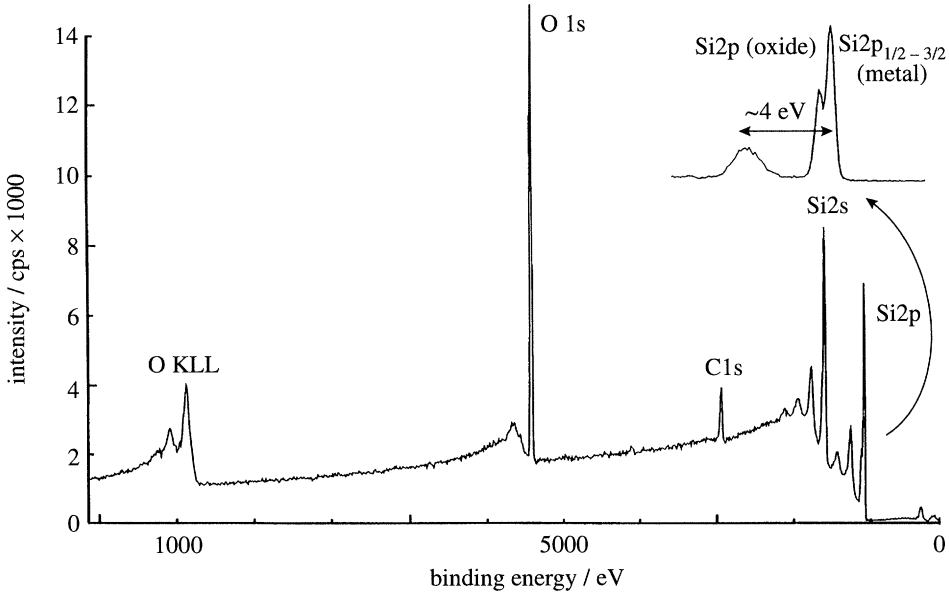

Figure 2. A typical X-ray photoelectron spectrum. The sample is a partially oxidized Si surface. Photoelectron lines are assigned to core levels and these and other features are discussed in the text. The inset shows the detail of the Si2p region.

3. Methods of imaging and selected area analysis in XPS

The following discussion is limited to those methods of imaging and selected area analysis which are commercially available or are viable as attachments to 'big science' devices such as synchrotron soft X-ray sources.

Early attempts at XPS imaging and selected area analysis have been summarized in the papers of Drummond *et al.* (1985) and Seah & Smith (1988).

Essentially, the methods for XPS imaging can be broken down into two main groups (Drummond 1992). In the first, the X-ray beam bombarding the specimen is localized, i.e. an X-ray probe (see figure 3). The second method is to flood the specimen with X-rays and then image part of the specimen surface by manipulating the photoelectrons in a controlled manner (see figures 4 and 5).

The X-ray probe based instruments are described first followed by the 'electron optical' methods. Prior to the description of the electron optically based methods there is a section on the role of the lens in XPS instrumentation which should prove helpful in understanding electron optical methods.

(*a*) *A focused X-ray probe using a focusing crystal monochromator*

Although X-ray focusing elements such as zone plates have only recently become available, focusing by means of crystals is well established. Crystal focusing was applied to selected area XPS in the mid 1980s (Chaney 1987). It is now claimed that an area as small as 10 μm in diameter can be illuminated with a relatively high flux of monochromatic X-rays (Larson & Palmberg 1994). The basic configuration of a small spot crystal monochromator is shown in figure 3*a*.

The size of the primary X-ray spot, using a conventional electron bombardment source, is the size of the electron beam. Small diameter electron beams are readily achieved but there are technological difficulties in producing a correspondingly small viable X-ray source. Firstly, there must be sufficient current in the beam to produce

PHILOSOPHICAL TRANSACTIONS OF THE ROYAL SOCIETY A MATHEMATICAL, PHYSICAL & ENGINEERING SCIENCES
PHILOSOPHICAL TRANSACTIONS OF THE ROYAL SOCIETY A MATHEMATICAL, PHYSICAL & ENGINEERING SCIENCES

Downloaded from rsta.royalsocietypublishing.org

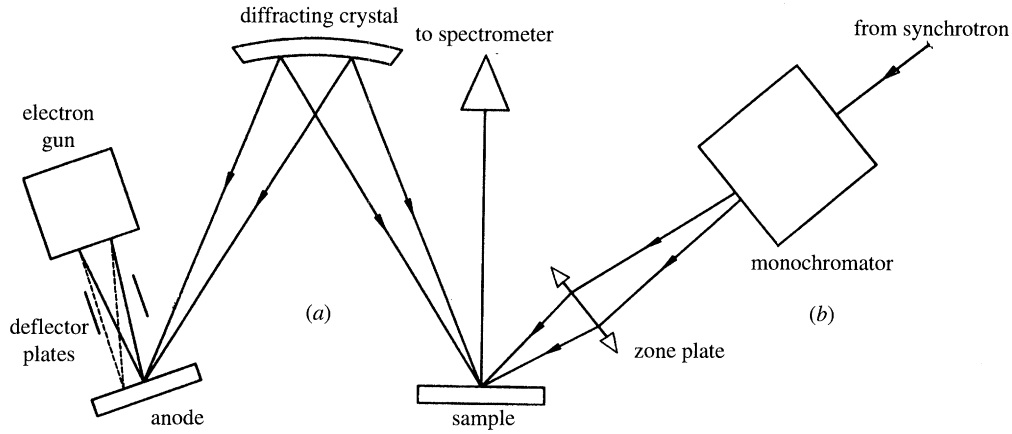

Figure 3. A composite schematic showing two approaches to a focused X-ray microprobe: (*a*) the point focusing monochromator (Larson & Palmberg 1994); (*b*) the zone plate focusing method (Ade *et al.* 1990).

a reasonable flux of X-rays and secondly the anode must be able to withstand the thermal loading produced by the electron beam. Larson & Palmberg (1994) claim anode loadings of 80 kW mm^{-2} and 1.2 kW mm^{-2} in spots of 4 μm and 250 μm diameter, respectively.

The image of the small X-ray source will be enlarged by the magnification of the monochromator, i.e. the relative positions of the source, diffracting crystal and X-ray focus on the Rowland circle (Witz 1969). Furthermore, there are aberrations which include an 'aperture' aberration, a 'chromatic' aberration (it must be remembered that the monochromator is a dispersive device), a diffraction aberration and imperfection aberrations, e.g. any imperfections in the crystal lattice planes and mechanical imperfections in the bending. Spherical bending is used in most point focusing monochromators with a large Bragg angle but it does give rise to some astigmatism which can be corrected by elliptical bending.

The monochromatic source of Larson & Palmberg (1994) is similar to previous monochromators used for XPS; it uses quartz crystals cut parallel to $10\bar{1}0$ bent elliptically in a Johann type configuration to monochromatize AlKα radiation. The appropriate Bragg angle is 78.5° and the diameter of the Rowland circle is 200 mm. The aperture defect would normally give rise to an aberrated disc of approximately 25 μm diameter from an individual crystal—clearly larger than the 10 μm claimed. However, the bending of the crystal causes a non-uniform spacing in the lattice planes which acts in such a way as to compensate for the aperture defect.

Larson & Palmberg (1994) scan the X-ray probe over the specimen surface by scanning the electron beam in the X-ray source. This causes the monchromator to lose its optimum focus, just as happens in a wavelength dispersive electron probe X-ray microanalyser. Various means for compensating this effect are available.

(*b*) *A focused X-ray probe using synchrotron radiation*

Recent advances made in X-ray optics, particularly those relevant to X-ray microscopy, have led to the development of an X-ray probe using monochromatized synchrotron soft X-radiation. Figure 3*b* shows a schematic of such an instrument (Ade *et al.* 1990). Ade and his colleagues use a spherical monochromator followed by

Downloaded from rsta.royalsocietypublishing.org

a focusing zone plate. The probe has a diameter of 0.3 μm and is scanned over the region of interest by scanning the specimen.

(*c*) *The role of the lens(es) in XPS instrumentation*

Figure 1*a* shows a lens between the sample and the energy analyser in a typical XPS instrument. The purpose of the lens is to focus the photoelectrons into the energy analyser and to retard them at the same time. Retardation of the electrons enhances the energy resolution of the analyser, as pointed out by Siegbahn *et al.* (1967). The distance between the specimen and the analyser is fixed and this imposes a restraint on the lens, i.e. whatever the kinetic energy of the electron selected by the analyser the lens must stay in focus.

Other constraints may apply to the lens, e.g. if the analyser is working at a fixed pass energy then the retardation must vary to maintain this pass energy—this is the fixed or constant analyser transmission/energy mode. Alternatively, it might be desired that the retardation is such that the retarded electrons have a fixed proportion of the kinetic energy of the emitted photoelectrons—the fixed retardation ratio mode. Finally, it is desirable that the magnification of the lens remains constant. To perform retardation, electrostatic lenses are used and if there are N constraints on the running of the lens then it should have a minimum of $N + 1$ independently variable electrodes.

(i) *Angular acceptances of lenses, etc.*

Suppose the analyser entrance aperture is the limiting field aperture in the system, then the area from which photoelectrons will be accepted will have a width of s as defined by the expression

$$s = D/M, \tag{3.1}$$

where D is the width of the aperture and M is the magnification of the lens. Further suppose that the transmission of the instrument is limited by the angular acceptance of the analyser. In this case the semi-angle of the photoelectron beam accepted from the specimen is given by the expression

$$\alpha_s = M\alpha_0/R^{1/2}, \tag{3.2}$$

where α_0 is the limiting half angle (analyser), M is the magnification and R the retarding ratio of the lens (i.e. if 1000 eV electrons enter the lens and 100 eV electrons leave then $R = 10$).

If $\alpha_0 = 0.14$ rad, $M = 3$ and $R = 40$ then the semi-angle accepted from the specimen is *ca.* 0.07 rad, provided there are no other limiting apertures. If M is increased to 10 for the same conditions then $\alpha_s \approx 0.22$ rad, i.e. a semi-angle of 12.5°. This argument would indicate that the magnification of the lens should be high to obtain a greater input of photoelectrons from the sample. However, expression (3.1) indicates that if the input slit has the same width then the area of sample from which photoelectrons are accepted is reduced. In fact, the number of photoelectrons $\sec^{-1}$ at the analyser is virtually the same in both cases.

In the case of the larger acceptance angle at the specimen, the effect of spherical aberration will be more significant as will be shown and, in addition, analysis in depth by angular dependence is degraded.

In reality, the energy analyser is likely to have different acceptance angles in the dispersive and non-dispersive planes. This is significant in 'standard' XPS but less important in most cases of spatially resolved XPS.

Downloaded from rsta.royalsocietypublishing.org

A discussion of the various arrangements of electron optical imaging XPS methods follows.

(*d*) *The sequential pixel by pixel method*

Expression (3.1) in § 3 *c* (i) showed that an area of diameter a on the specimen could be selected by an aperture of diameter Ma by a lens of magnification M. The system is essentially an electron microprobe in reverse and the approach is commonly known as the 'virtual microprobe'. By placing deflection plates between the specimen and the lens it is possible to scan the virtual probe and form an image of the distribution of an element or a particular chemical state as well as detect a range of energies simultaneously. Alternatively, a selected area analysis can be carried out. Such systems based on electrostatic lenses have been described by Yates & West (1983), Seah & Smith (1988) as well as a commercial version by Drummond *et al.* (1992).

Systems using electrostatic lenses suffer from large spherical aberration effects which limit their resolution. Some degree of success in compensating for spherical aberration in the electrostatic lens has been achieved (Read 1982) and this was incorporated in an aberration-compensated input lens which had a large angular acceptance. However, it has been shown (Read & Drummond 1984, unpublished work) that to fully compensate a lens system for spherical aberration as well as meeting the constraints outlined in § 3 *c* is virtually impossible.

The introduction of a magnetic lens into an imaging system (Walker 1991) has made significant advances possible and a schematic of a modern instrument (Kratos AXIS HSi) is shown in figure 4. Two probe forming lenses are incorporated, one electrostatic (E) and the other a magnetic lens (ML) of the single pole-piece type (Mulvey 1982). These are followed by an electrostatic retarding lens (LR) after the area defining aperture (D). Having the retarding lens decoupled from the probe lens eases the constraints on the lenses. The electrostatic probe lens, the aberrations of which have been discussed by Drummond *et al.* (1992), is used for large fields of view in a search mode while the magnetic lens with its lower aberrations is used for high resolution mapping and selected area analysis. The spherical aberration limits on the magnetic lens system have been outlined by Walker (1991).

An advantage of the pixel by pixel approach is that each point on the specimen surface can be addressed by the voltages applied to the deflection plates (DP). This means that after an image has been acquired selected areas of interest can selected and detailed 'point' analyses made.

(*e*) *The line by line or E–x approach*

The hemispherical electrostatic energy analyser (which is almost universally used in XPS) focuses in both the dispersive and non-dispersive planes. It is therefore possible to form a line image in the non-dispersive direction and at the same time record the spectrum in the dispersive plane associated with each point in the line—hence the E–x terminology to describe the method. The line on the specimen corresponds to a lens demagnified analyser entrance slit cf. the virtual microprobe approach; the lens being a five electrode electrostatic lens of variable magnification. The energy information is captured by a detector array across the output focal plane of the analyser. The E–x information is stored and the sample is then moved incrementally in the y direction so that a whole matrix of E–x information is built up (Gelius *et al.* 1990).

Downloaded from rsta.royalsocietypublishing.org

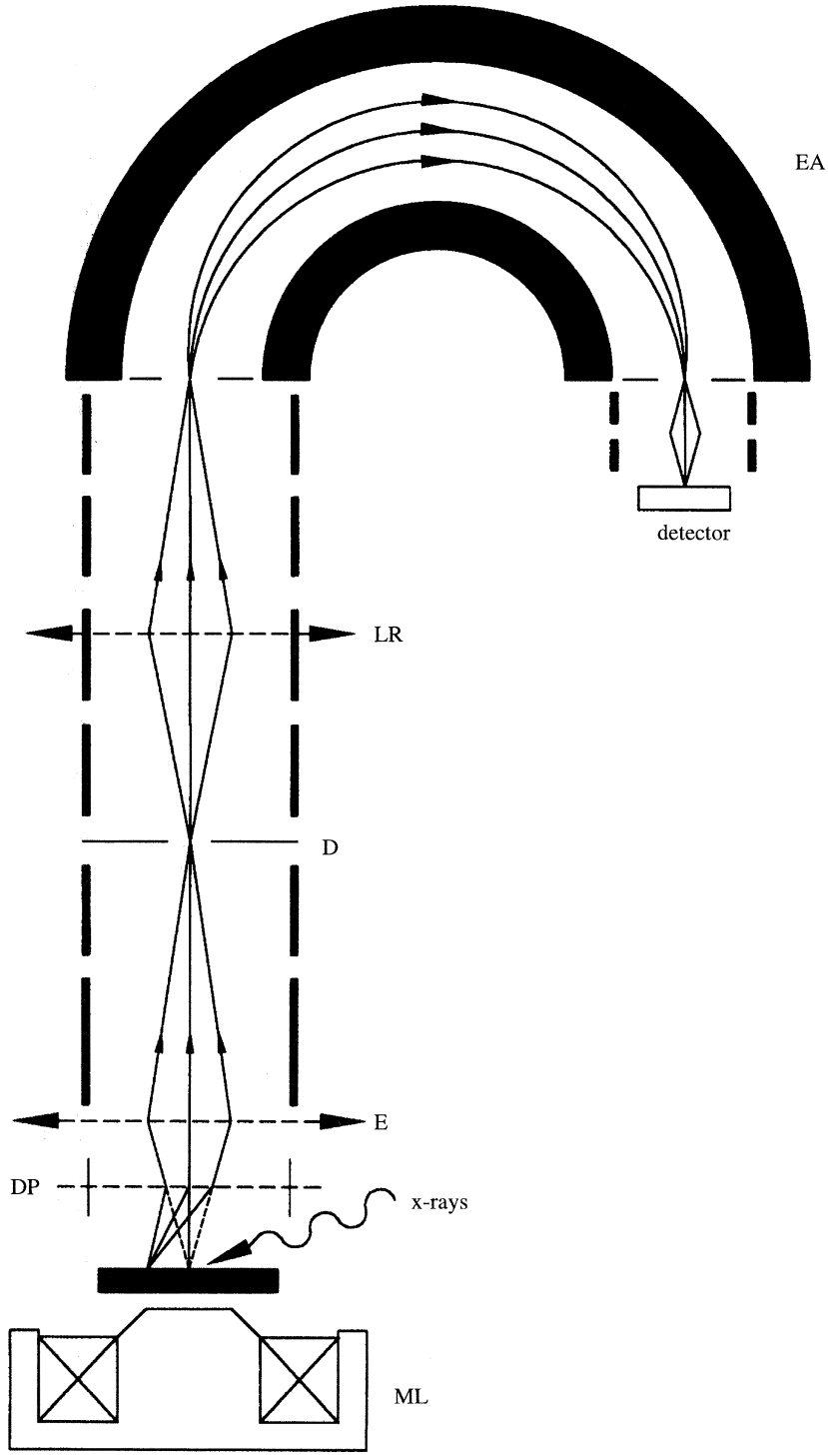

Figure 4. A schematic of the pixel by pixel scanning electron optical method of imaging XPS (after Drummond 1992). Note that the main focusing action of the snorkel lens is in front of the physical structure of the lens.

PHILOSOPHICAL TRANSACTIONS OF THE ROYAL SOCIETY A MATHEMATICAL, PHYSICAL & ENGINEERING SCIENCES
PHILOSOPHICAL TRANSACTIONS OF THE ROYAL SOCIETY A MATHEMATICAL, PHYSICAL & ENGINEERING SCIENCES

Downloaded from rsta.royalsocietypublishing.org

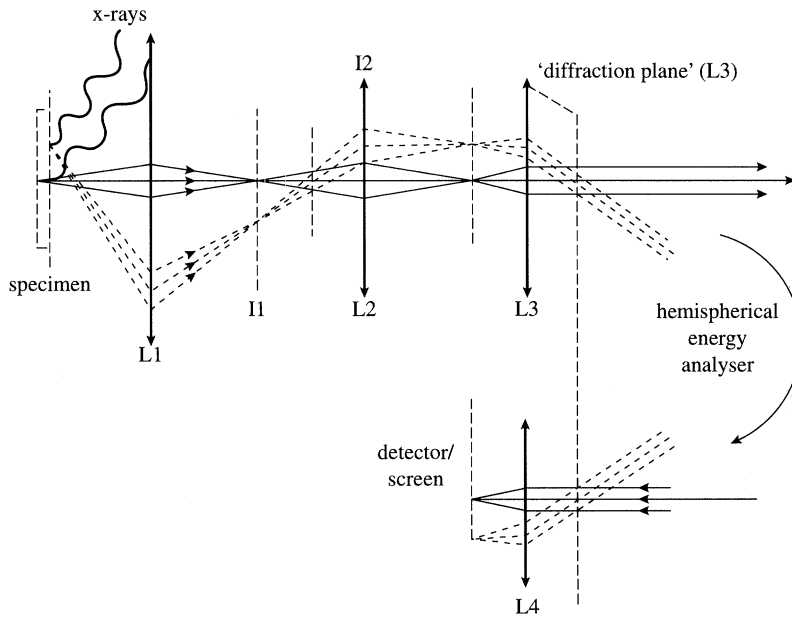

Figure 5. A parallel imaging electron optical method of imaging XPS. Drawn by Drummond (1992) after Coxon *et al.* (1990). Reproduced by courtesy of *Microscopy and Analysis* (March 1992).

The E–x information can then be unfolded to give detailed spatial information at different photoelectron energies. A single E–x line can provide information on linear structures.

(*f*) *The parallel imaging mode*

An imaging method which can gather all the spatial information simultaneously has some advantages over the point by point or line by line approach. Such a method has been described by Coxon *et al.* (1990) and the basic optics of the system are shown schematically in figure 5.

It will be seen that there are three lenses preceding the analyser. The first two (L1 and L2) provide two stages of magnification, each magnifying by a factor of 4, or greater, to give an overall magnification of 16–64× at I2. The third lens (L3) is so arranged that the distance from the image of L2 to L3 is equal to the focal length of L3. The object plane of the analyser now coincides with the diffraction plane of L3. This means that L3 can code spatial information in the image (I2) into angular information—each point producing parallel trajectories into the analyser at a distinct angle. These parallel rays are energy analysed and can either be directly collected to give a photoelectron spectrum of the whole of the viewed area or they pass through another lens (L4) which decodes the angular information back into spatial information where it is displayed in a channel plate intensifier and subsequently recorded.

This latter mode produces a map of a particular energy, i.e. of an element or chemical state. In order to produce a selected area analysis, i.e. from a point on the image, an aperture system is placed at a suitable point in the lens transfer system consisting of L1 and L2. L1 and L2 are einzel type lenses while L3 provides the retardation into the analyser. In reality, the system (the Escascope, manufactured by

Downloaded from rsta.royalsocietypublishing.org

VG Scientific Ltd) may have more lens elements than shown in figure 5 but this does not affect the understanding of the instrument. Recently, a magnetic lens has been used in the instrument which, not unexpectedly, improves the performance. Both the AXIS (figure 4) and the Escascope depend on immersion lenses and an excellent discussion on such lenses (albeit electrostatic) is given by Rempfer & Griffith (1991).

(*g*) *The magnetic projection photoelectron spectromicroscope*

No discussion on imaging XPS would be complete without mention of the photoelectron spectromicroscope. This novel instrument (Beamson *et al.* 1981) places the specimen in a strong axial magnetic field (7 T) where it is illuminated by UV- or X-radiation. Photoelectrons are emitted and spiral round the magnetic field lines with a small radius. As the field strength falls away from the high field region the electrons follow larger radii and the magnification is given by the ratio of larger to smaller radius and is typically 100×. The image is always in focus as this is, essentially, a point projection method.

In order to image a particular photoelectron energy an ingenious band-pass energy filter has been designed which will work in a magnetic field (Turner *et al.* 1986). UV photoelectron images with a resolution of less than or equal to 1 μm have been produced; X-ray photoelectron images are slightly worse, as theory predicts.

(*h*) *Depth information*

The easiest way to obtain spatial information at different depths is to uniformly ion etch away the surface. Provided differential sputtering rates are not serious, information should be available from a few nm to tens of nm below the surface.

Taking measurements at two different angles between the specimen and the spectrometer, i.e. 'normal' and 'grazing incidence, is used in conventional XPS to obtain non-destructive depth information—albeit of a limited depth range. Under grazing incidence the escape depth of a given photoelectron line samples a much lower actual depth than it does at normal incidence. However, the method is difficult to apply to imaging and selected area XPS because of foreshortening and allied effects.

The use of different energy X-ray sources alters the energy, and hence the escape depth of a given photoelectron (line), and can be used to probe limited depths non-destructively. It is easier to apply to spatially resolved XPS.

(*i*) *A cautionary note on image information*

Assessing the resolution of image can be subjective and the resolution of XPS images is generally measured by observing a sharp edge and measuring the distance between untreated signal intensities of 84% and 16%. In some cases this is relaxed to 80–20%. However, if the optics of the instrument are seriously aberrated so as to produce a wide 'skirt' of 10% intensity, this will generally not be observed in the image. It will nevertheless have serious repercussions in a selected area mode which will not give an accurate analysis of the area due to 'over-lap' effects from adjacent areas. It is the author's view that in assessing the performance of a spatially resolving XPS instrument, the quality of the analytical information should have preference over the appearance of the image.

4. Applications of spatially resolved XPS to semiconductors

As has been mentioned previously, the spatial resolution of commercial XPS instruments is 5–30 μm (as a conservative estimate), which is in excess of the smallest

PHILOSOPHICAL TRANSACTIONS OF THE ROYAL SOCIETY A MATHEMATICAL, PHYSICAL & ENGINEERING SCIENCES
PHILOSOPHICAL TRANSACTIONS OF THE ROYAL SOCIETY A MATHEMATICAL, PHYSICAL & ENGINEERING SCIENCES

Downloaded from rsta.royalsocietypublishing.org

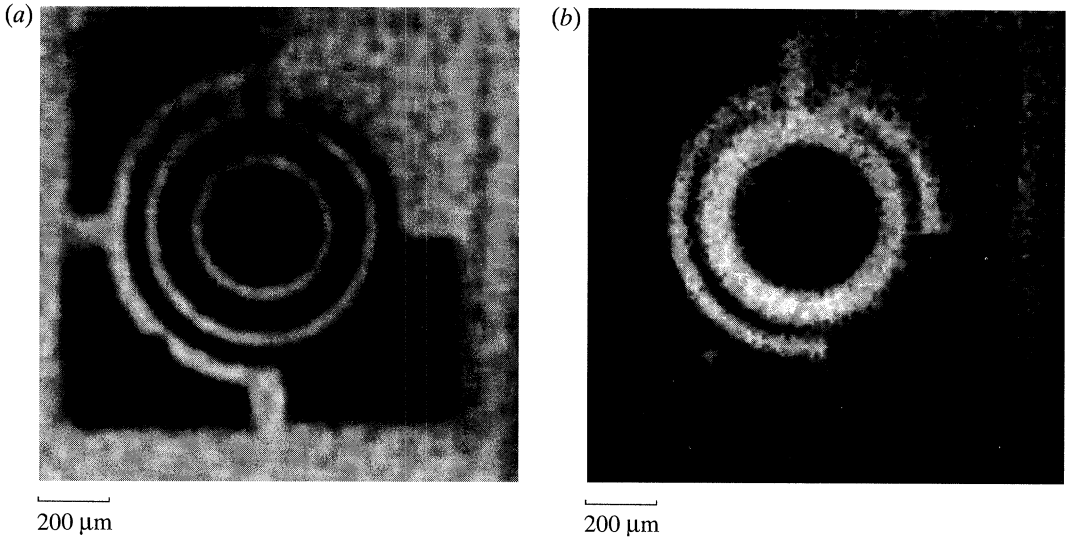

Figure 6. (*a*) An XPS image of a power transistor formed using Si2p (metal) photoelectrons (binding energy *ca.* 100 eV). (*b*) As (*a*) but using the Si2p (oxide) photoelectrons (binding energy *ca.* 104 eV). The central and peripheral areas that are dark in both images are covered in photo-resist.

semiconductor structures. The X-ray probe of Ade *et al.* (1990) has shown sub-micron resolution (0.3 μm) on a fabricated semiconductor sample.

Using the virtual microprobe chemical state images, the Si2p photoelectrons of Si (metal) and Si (oxide) of a relatively large power transistor are shown in figure 6. Smaller structures such as tracks, etc., can be imaged but show relatively unexciting chemistry.

A complex study of semiconductor materials/structures was initiated by a desire to convert depth information into spatial information by the process of ion bevelling (McPhail & Dowsett 1988). A sample of a series of alternating layers of Si metal and $Si_{0.75}Ge_{0.25}$ alloy each 30 nm thick was bevel etched with 4 keV O_2^+ ions at a bevel angle of 10^{-4} rad, producing a magnification of the layers on the bevelled surface of 10^4 times. Thus a layer 30 nm deep produced a surface stripe 300 μm wide. The ion dose used in the bevelling was sufficient to allow an equilibrium altered surface layer to be formed.

The striped etched surface, both with the altered layer present and with it chemically removed, were examined with spatially resolved XPS. The altered surface showed heavy oxidation, the Si layers being covered with SiO_2 and the SiGe layers being covered with a layer of mixed SiO_2 and GeO_2. With the altered layer removed by an HF etch, the striped appearance of the surface was preserved but the structure was more complicated than expected. The Si stripes showed that an oxide layer, in excess of that expected, remained. The SiGe layers were rather surprisingly capped with mainly oxidized Ge, some metallic Ge but very little Si oxide and no Si. In addition the Ge–Ge (oxide) stripes were much wider than the Si–Si (oxide) stripes—see the spatially resolved linescan shown in figure 7 (Drummond *et al.* 1992).

In order to understand some of these anomalies a comprehensive depth profiling study was made of bulk $Si_{0.83}Ge_{0.17}$ with a modified layer produced by normal incidence bombardment with 4 keV or 8 keV O_2^+ ions (Dowsett *et al.* 1993). Transmission electron microscopy (TEM), AES, SIMS and XPS were all used to depth profile the

Downloaded from rsta.royalsocietypublishing.org

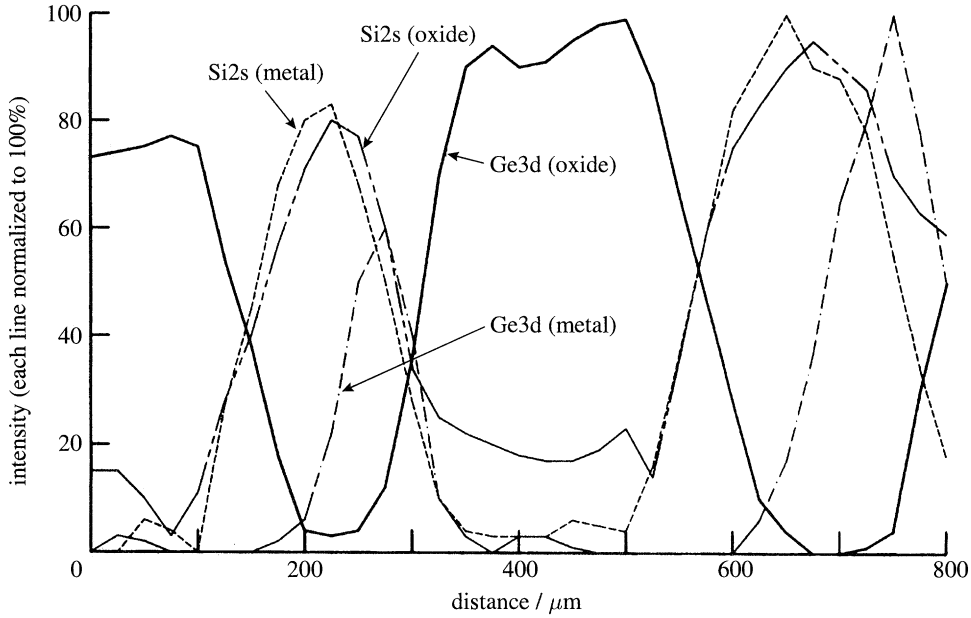

Figure 7. A linescan across a bevel etched Si–$Si_{0.75}Ge_{0.25}$ multilayer sample (at right angles to the exposed stripes). After Drummond *et al.* (1992). Courtesy American Institute Physics.

altered layer. Some differences were recorded in the profiles but they all showed a migration of metallic Ge towards the back of the altered layer with the TEM work showing more than one Ge layer. Evidence suggests a model in which the Ge segregates to form a virtually 100% pure layer of Ge metal behind a layer consisting of SiO_x and SiO_2. For some reason, the Ge layer becomes unstable and forms a band of discrete nodules. This exposes the underlying SiGe alloy to the Si oxide layer and a new Ge layer starts to build up. Is interesting to compare this process with the thermal oxidation of SiGe studied by LeGoues *et al.* (1989).

The XPS depth profile (figure 8) is not as detailed as the TEM cross section but it is believed that atomic mixing during profiling and surface oxidation of the Ge during instrument transfer have complicated matters.

The bevel etching of the SiGe alloy also shows that there is a significant lateral migration of the Ge which results in the uneven width of Ge and Si stripes (figure 7). Moreover, the HF etch appears to only partially remove the altered layer on the stripes.

The segregation of Ge in 50:50 SiGe alloys by oxygen ion implantation has been studied by Castle *et al.* (1993) who have advanced thermodynamic reasons for the Ge segregation in place of the empirical models formerly advanced.

The above results show that structures containing SiGe alloys are unsuitable for bevel etching and they also illustrate some of the difficulties in interpreting the chemistry of small scale structures that have been fabricated with active species and/or have had chemical post-treatment. On the other hand they can suggest improvements in manufacturing.

The ability of spatially resolved XPS to show such intricate chemistry has not, as yet, had the impact on the investigation of semiconductors as might be expected. However, AES and SIMS, with their high spatial resolution, (less than 0.1 μm) have become established—especially as semiconductors are resistant to invasive probes of

Downloaded from rsta.royalsocietypublishing.org

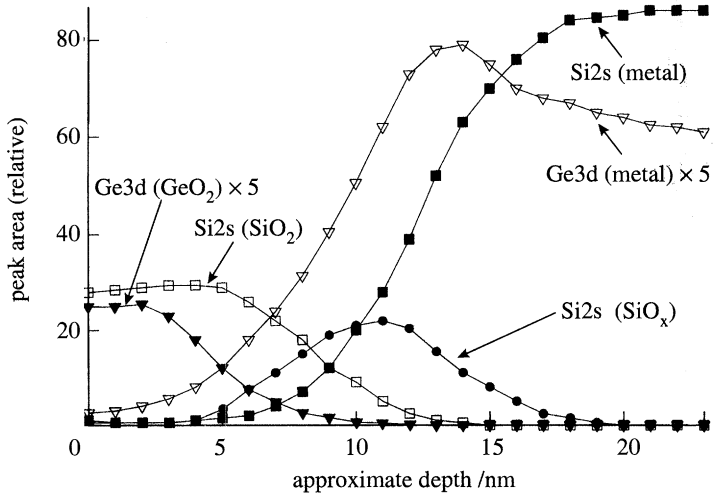

Figure 8. A depth profile through the altered layer of a multilayer Si–$Si_{0.83}Ge_{0.17}$ bulk sample. After Dowsett *et al.* (1993). Courtesy J. Wiley & Sons.

electrons and ions (cf. polymers where much damage is caused by such probes as compared with X-rays giving XPS a pronounced advantage). Moreover, experienced users have become adept at extracting what chemical information can be gleaned from AES and SIMS. An example of this is afforded by the work of Kazmerski (1993) who has used 'difference Auger spectra' and SIMS to show differences in H and O content in grain boundaries in polycrystalline Si. It is expected that the recent availability of Auger probes in magnetic lens based high resolution XPS instrumentation will address this imbalance.

5. Possible improvements in spatially resolved XPS

It must now be asked whether the spatial resolution of XPS can be improved to observe those semiconductor structures already in existence and those likely to be developed in the near future. Areas in conventional instrumentation which can be enhanced include improvements in the intensity of X-ray sources and in the electron optics of collecting lenses as well as in the transmission of the energy analyser.

The anode thermal loads in conventional electron bombardment sources are approaching the theoretical limit and it seems likely that improved synchrotron radiation soft X-ray sources may be the solution. Magnetic lenses together with improved parallel imaging may effect some improvement, as could aberration corrected energy analysers. Skoczylas *et al.* (1991) have suggested a method eliminating aberrations in emission microscopes but attempts to remove all electron optical defects in the past have proved disappointing.

While the evolution of the instruments described in § 3 may produce significant improvements using the approaches outlined in the previous paragraph it is worthwhile examining some of the less conventional avenues to ultra high spatial resolution XPS. Three interesting methods are being actively persued, two of which are directly related to XPS.

X-ray photoelectron diffraction and holography (Fadley 1993; Tonner 1991) offers information on an atomic scale but this simple statement is misleading. The diffraction information is derived from a large averaged-out structure and gives information

Downloaded from rsta.royalsocietypublishing.org

only from single crystals or such crystals with regular structured adsorbates. The only way to localize the information is to use an X-ray probe or an electron optical technique such as those described in § 3. As Tonner (1991) points out, it is the analogue of selected area electron diffraction in the TEM.

Pijper & Kruit (1991) have shown that it is possible to carry out photoelectron spectroscopy using a high energy electron beam as the exciting source—the electrons acting as 'virtual' photons. An incident electron may interact with an atom of a thin specimen causing the ejection of a photoelectron. By using two electron spectrometers working in coincidence mode, one to measure the energy of the photoelectron and the other to determine the kinetic energy of the photoelectron, it is possible to determine the binding energy of the ejected photoelectron. The advantage of using electron beam excitation is the high spatial resolution that can be achieved.

Finally, the conventional electron emission microscope has been used by Harp *et al.* (1990) in conjunction with a variable energy photon source to study X-ray absorption near edge structure (XANES). The emission of low energy photoelectrons (less than or equal to 2 eV) reflects X-ray absorption; as the absorption changes so does the yield of the low energy photoelectrons. The emission microscope can give a high spatial resolution (10 nm) using 2 eV electrons and so the XANES data can be mapped out. Harp *et al.* (1990) have shown various valence states of Si using the Si2p edge on a Si sample with a variable thickness of oxide. The data is not dissimilar to XPS data.

6. Conclusions

Although spatially resolved XPS is constantly improving it is doubtful that it will be capable of resolving the smallest semiconductor structures in the near future. It is felt that AES, SIMS and proximal microscopies will be at an advantage for probing such structures and surfaces. However, when the chemistry involved in the surface is complex XPS offers unique capabilities.

The author thanks his colleagues Dr Simon Page and Mr Mike Greenbank for their encouragement and help in preparing this paper. They are in no way to blame for errors of fact or omission. Thanks are also due to Kratos Analytical for permission to publish this work.

References

Ade, H. W., Kirz, J., Hulbert, S. L., Johnson, E. D., Anderson, E. & Kern, D. 1990 X-ray spectromicroscopy with a zone plate generated microprobe. *Appl. Phys. Lett.* **56**, 1841–1843.

Beamson, G., Porter, H. Q. & Turner, D. W. 1981 Photoelectron spectromicroscopy. *Nature*, **290**, 556–561.

Briggs, D. & Riviere, J. C. 1990 Spectral interpretation. In *Practical surface analysis* (ed. D. Briggs & M. P. Seah), vol. 1, 2nd edn, pp. 85–141. Chichester: Wiley.

Castle, J. E., Liu, H. D. & Saunders, N. J. 1993 A study of oxygen implanted $Si_{0.5}Ge_{0.5}$ alloy by XPS and thermodynamic analysis. *Surf. Interface Analysis* **20**, 149–154.

Chaney, R. L. 1987 Recent developments in spatially resolved ESCA. *Surf. Interface Analysis* **10**, 36–47.

Coxon, P., Krizek, J., Humpherson, M. & Wardell, I. R. M. 1990 Escascope—a new imaging photoelectron spectrometer. *J. Electron Spectrosc. Rel. Phenom.* **52**, 821–836.

Dowsett, M. G., James, D. M., Drummond, I. W., El Gomati, M. M., El Bakush, T. A., Street, F. J. & Barlow, R. D. 1993 Redistribution of Ge in the SIMS altered layer during normal incidence O_2^+ bombardment of SiGe alloy material. In *SIMS VIII.* (ed. A. Benninghoven, K. G. S. Janssen, J. Tumpner & H. W. Werner), pp. 359–362. Chichester: Wiley.

Downloaded from rsta.royalsocietypublishing.org

Drummond, I. W., Cooper, T. A. & Street, F. J. 1985 Four classes of selected area XPS (SAXPS): an examination of methodology and comparison with other techniques. *Spectrochim. Acta*, B **40**, 801–810.

Drummond, I. W., Street, F. J., Ogden, L. P. & Surman, D. J. 1991 AXIS: an imaging X-ray photoelectron spectrometer. *Scanning* **13**, 49–163.

Drummond, I. W. 1992 Imaging XPS: the different methods explained. *Miscrosc. Microanal.* **28**, 29–32.

Drummond, I. W., Dowsett, M. G., James, D. M. & Street, F. J. 1992 High-resolution depth profiling of semiconductor structures: preliminary results. *J. Vac. Sci. Technol.* A **10**, 2897–2901.

Fadley, C. S. 1993 Diffraction and holography with photoelectrons and Auger electrons: some new directions. *Surf. Sci. Rep.* **19**, 231–264.

Ferguson, I. F. 1989 *Auger microprobe analysis.* Bristol: Adam Hilger.

Gelius, U., Wannberg, B., Baltzer, P., Fellner-Felegg, H., Carlsson, G., Johansson, C.-G., Larsson, J., Munger, P. & Vegefors, G. 1990 A new ESCA instrument with improved surface sensitivity, fast imaging properties and excellent energy resolution. *J. Electron Spectrosc. Rel. Phenom.* **52**, 747–785.

Harp, G. R., Han Zhi-Lan & Tonner, B. P. 1990 Spatially-resolved X-ray absorption near-edge spectroscopy of silicon in thin silicon-oxide films. *Physica Scripta*, T **31**, 23–27.

Jenkin, J. G., Leckey, R. C. G. & Liesegang, J. 1977 The development of X-ray photoelectron spectroscopy: 1900–1960. *J. Electron Spectrosc. Rel. Phenom.* **12**, 1–35.

Jenkin, J. G., Riley, J. D., Liesegang, J. & Leckey R. C. G. 1978 The development of X-ray photoelectron spectroscopy (1900–1960): a postscript. *J. Electron Spectrosc. Rel. Phenom.* **14**, 477–485.

Kazmerski, L. L. 1993 Micro- to nano-characterization of semiconductor grain boundaries. *Surf. Sci. Rep.* **19**, 169–189.

Larson, P. E. & Palmberg, P. W. 1994 Scanning and high resolution X-ray photo electron spectroscopy and imaging. European Patent Application. Publication no. 0 590 308 A2, European Patent Office., 16.

LeGoues, F. K., Rosenberg, R., Nguyen, T., Himpsel, F. & Meyerson, B. S. 1989 Oxidation studies of SiGe. *J. Appl. Phys.* **65**, 1724–1728.

McPhail, D. S. & Dowsett, M. G. 1988 Bevelling-etch-imaging A novel technique for revealing thin layer structures. In *SIMS VI* (ed. A. Benninghoven, A. M. Huber & H. W. Werner). New York: Wiley.

Mulvey, T. 1982 Unconventional lens design. In *Magnetic electron lenses* (ed. P. W. Hawkes), pp. 359–415. Berlin: Springer.

Pijper, F. J. & Kruit, P. 1991 Detection of energy-selected secondary electrons in coincidence with energy loss events in thin carbon foils. *Phys. Rev.* **44**, 9192–9200.

Read, F. H. 1982 Charged particle spectrometer. US Patent No. 4,358,680, USA Patent and Trademark Office.

Rempfer, G. F. & Griffith, O. H. 1991 The resolution of photoelectron microscopes with UV, X-ray and synchrotron radiation sources. *Ultramicroscopy* **36**, 273–300.

Seah, M. P. & Smith, G. C. 1988 Concept of an Imaging XPS system. *Surf. Interface Analysis* **11**, 69–79.

Siegbahn, K., Nordling, C. N., Fahlman, A., Nordberg, R., Hamrin, K., Hedman, J., Johansson, G., Bermark, T., Karlsson, S. E., Lindgren, I. & Lindberg, R. 1967 *ESCA: atomic, molecular and solid state structure studied by means of electron spectroscopy.* Uppsala: Almqvist & Wiksells.

Skoczylas, W. P., Rempfer, G. R. & Griffith, O. H. 1991 A proposed modular imaging system for photoelectron and electron probe microscopy with aberration correction, and for mirror microscopy and low energy electron microscopy. *Ultramicroscopy* **36**, 252–261.

Stix, G. 1995 Toward 'point one.' *Scient. Am.* **272**, 72–77.

Tonner, B. P. 1991 Photoelectron holography for high resolution spectromicroscopy. *Ultramicroscopy* **36**, 130–141.

Downloaded from rsta.royalsocietypublishing.org

Turner, D. W., Plummer, I. R. & Porter, H. Q. 1986 Electron energy analysis in emission microscopy. *Ann. N.Y. Acad. Sci.* **483**, 354–371.

Walker, A. R. 1991 A charged particle energy analyser. European patent specification, Publication no. 0 243 060 B1, European Patent Office.

Watts, J. F. 1994 X-ray photoelectron spectroscopy. *Vacuum* **45**, 653–671.

Witz, J. 1969 Focusing monochromators. *Acta Crystallogr.* A **25**, 30–42.

Woodruff, D. P. & Delchar, T. A. 1986 *Modern techniques of surface science*. Cambridge University Press.

Yates, K. & West, R. H. 1983 Small area X-ray photoelectron spectroscopy. *Surf. Interface Analysis* **5**, 217–221.

Discussion

R. M. D. Bryson (*Department of Materials Science, University of Surrey, UK*). When managing, on line, with a particular photoelectron line, is there a problem with differential charging in different sample regions?

I. W. Drummond. If a sample consists of a mixture of conducting and non-conducting areas then there is a potential problem of differential charging in the on-line image. In the 'pseudo' monochromatic mode (i.e. the sample is flooded with X-rays produced from a conventional electron bombardment X-ray source which emits Bremsstrahlung in addition to the characteristic line) then an insulated sample usually charges up a few volts positive with respect to earth. At this point sufficient scattered and secondary low energy electrons from areas round the sample are attracted to the sample and a stable condition is achieved. If the conducting areas are deliberately earthed then differential charging will occur. If the conducting areas are allowed to float then the problem can be overcome, particularly in instruments with magnetic lenses, where a low energy electron source can be placed in the magnetic field in such a way to allow the low energy electrons to spiral along field lines to cause very effective neutralization at the correct point on the sample. Allowing differential charging to take place is a useful diagnostic technique for identifying conducting areas.

With a pure monochromatic X-ray source of X-rays there are usually insufficient secondary electrons to effect a stable neutralization so the auxiliary low energy electron source is essential in overcoming differential charging. In the case of a high-quality dispersive monochromator of the type used by Larson & Palmberg (1994) a rather subtle photoelectron line shift can occur. As the primary electron beam in the X-ray source is rastered (see figure 3*a*) so the effective configuration of the monochromator is changed and as a consequence the energy band of selected X-rays changes. The change in the emitted photoelectron energy is compensated for by altering the energy selection of the analyser in sympathy with the rastering.

PHILOSOPHICAL TRANSACTIONS OF THE ROYAL SOCIETY A MATHEMATICAL, PHYSICAL & ENGINEERING SCIENCES

PHILOSOPHICAL TRANSACTIONS OF THE ROYAL SOCIETY A MATHEMATICAL, PHYSICAL & ENGINEERING SCIENCES

Downloaded from rsta.royalsocietypublishing.org

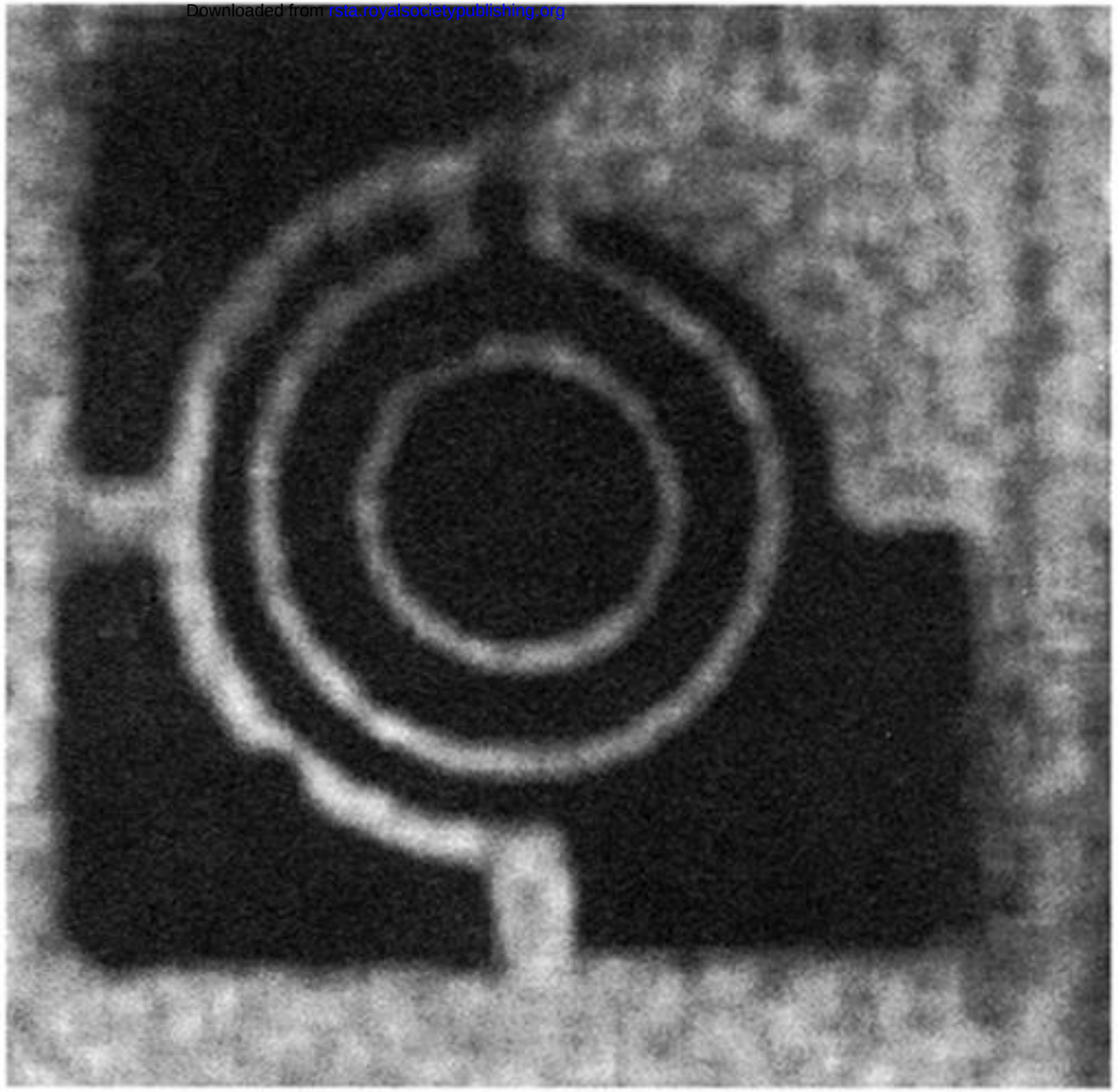

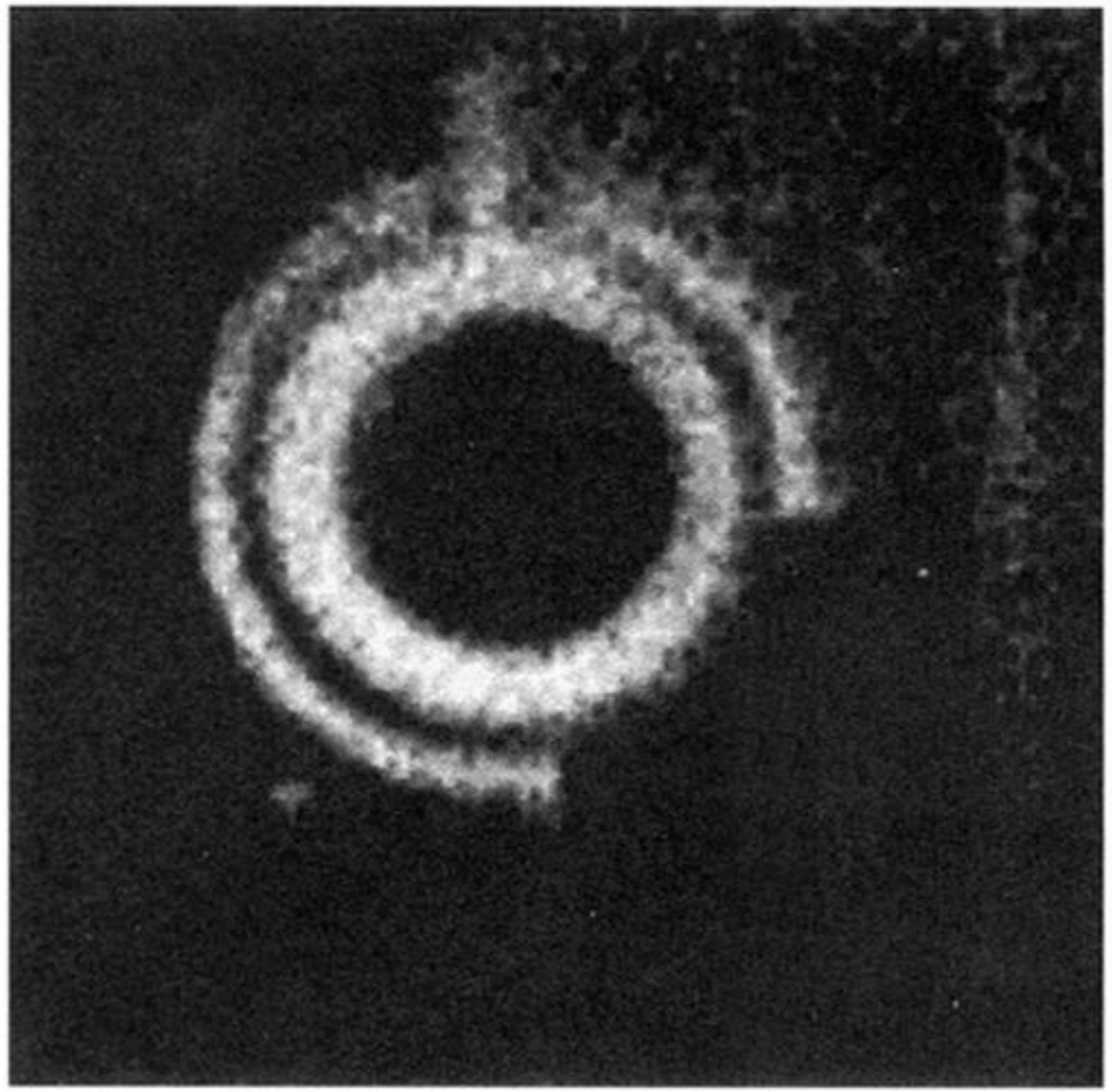

Figure 6. (*a*) An XPS image of a power transistor formed using Si2p (metal) photoelectrons (binding energy *ca.* 100 eV). (*b*) As (*a*) but using the Si2p (oxide) photoelectrons (binding energy *ca.* 104 eV). The central and peripheral areas that are dark in both images are covered in photo-resist.

PHILOSOPHICAL TRANSACTIONS OF THE ROYAL SOCIETY A MATHEMATICAL, PHYSICAL & ENGINEERING SCIENCES